Journal of ELECTRONIC MATERIALS, Vol. 47, No. 8, 2018
https://doi.org/10.1007/s11664-018-6273-y

TOPICAL COLLECTION: ELECTRONIC MATERIALS FOR RENEWABLE ENERGY APPLICATIONS

Comparative Analysis of Reduced-Rule Compressed Fuzzy Logic Control and Incremental Conductance MPPT Methods

EKREM KANDEMIR,[1,2,4] SELIM BOREKCI,[3] and NUMAN S. CETIN[2]

1.—TUBITAK National Observatory, Antalya, Turkey. 2.—Solar Energy Institute, Ege University, Izmir, Turkey. 3.—Department of Electrical and Electronics Engineering, Akdeniz University, Antalya, Turkey. 4.—e-mail: ekremkdemir@gmail.com

Photovoltaic (PV) power generation has been widely used in recent years, with techniques for increasing the power efficiency representing one of the most important issues. The available maximum power of a PV panel is dependent on environmental conditions such as solar irradiance and temperature. To extract the maximum available power from a PV panel, various maximum-power-point tracking (MPPT) methods are used. In this work, two different MPPT methods were implemented for a 150-W PV panel. The first method, known as incremental conductance (Inc. Cond.) MPPT, determines the maximum power by measuring the derivative of the PV voltage and current. The other method is based on reduced-rule compressed fuzzy logic control (RR-FLC), using which it is relatively easier to determine the maximum power because a single input variable is used to reduce computing loads. In this study, a 150-W PV panel system model was realized using these MPPT methods in MATLAB and the results compared. According to the simulation results, the proposed RR-FLC-based MPPT could increase the response rate and tracking accuracy by 4.66% under standard test conditions.

Key words: PV model, maximum-power-point tracking, incremental conductance, fuzzy logic control

INTRODUCTION

Renewable energy sources have been a major research topic in recent years, especially because of environmental issues such as pollution and global warming.[1] Photovoltaic (PV) energy is one of the most promising renewable energy sources. It is clean, inexhaustible, and free to harvest.[2] PV cells and panels have nonlinear electrical characteristics, and this characteristic is dependent on environmental conditions such as solar irradiance and ambient temperature. Therefore, all PV panels have power characteristic curves such that the maximum power is obtained when an impedance with a particular magnitude or load is connected. This impedance point is obtained only at a single operating point given by a particular voltage and current, called the maximum-power point (MPP), which varies considerably with both the solar irradiance and temperature.[1]

This forces researchers to develop a mechanism for determining the actual MPP depending on environmental changes. Therefore, maximum-power-point tracking (MPPT) algorithms have been utilized to emulate the unique impedance or load such that the the maximum achievable power can be extracted from a PV panel or system. MPPT methods direct the operating point of the PV system toward the MPP by controlling the power circuit of the PV system such that the operating point matches the maximum point of the contained PV panels. MPPT is a very important problem in PV systems, since extraction of the maximum achievable power from PV systems is of great value and importance.[3]

(Received October 25, 2017; accepted March 29, 2018; published online April 25, 2018)

In literature, many classical methods and controllers have been designed and widely implemented to track the MPP.[4–6] However, the different methods in actual use present different advantages as well as disadvantages such as slow response rate, energy loss, oscillations, etc.[7] Methods for MPPT can be classified into two main categories. The first includes classical or conventional techniques such as perturb and observe (P&O), incremental conductance (Inc. Cond.), hill climbing, fractional short-circuit voltage, and fractional short-circuit current, while the second category includes intelligent MPPT techniques, which are more versatile and capable than conventional techniques but also more complex.[1,3,8,9] Intelligent MPPT techniques include particle swarm optimization (PSO), fuzzy logic control (FLC)-based techniques, artificial neural network (ANN)-based techniques, and metaheuristic-based techniques.[3]

Various conventional and intelligent MPPT methods have been proposed to track the MPP, including adaptive P&O-modified Inc. Cond., particle swarm optimization (PSO), fuzzy logic control (FLC), and artificial neural network (ANN) approaches. These methods vary in terms of convergence speed, oscillations around the MPP, implementation complexity, cost, and electronic equipment requirements.[10–13] The P&O and hill climbing methods are very similar, as both require perturbation of some control variable to determine the tracking direction. This control variable could be the voltage, current, or duty ratio.[14] The Inc. Cond. method is derived from the same basis as the hill climbing and P&O methods but is based on a comparison of how the voltage and current change. This method is widely preferred and is an important technique in literature due to its good tracking performance and environmental adaptability.[15–18] The Inc. Cond. method is more robust to measurement noise compared with the P&O method because the control decision depends on two distinct variables.[19] Disturbance observations and incremental conductance are two of the most popular methods, being easy to implement in any digital controller and offering good approach to the MPP, but they exhibit oscillations around the MPP that cause serious energy loss and they fail to track the global MPP in partial shading conditions.[20] To avoid these drawbacks, intelligent MPPT techniques are generally preferred in literature.

The introduction of intelligent MPPTs for PV systems is highly promising. These methods achieve good performance in partial shading conditions, fast response with no overshoot, and less fluctuations.[13] One of the most widely used intelligent techniques is the fuzzy logic control (FLC)-based MPPT method, offering fast tracking ability and improved efficiency of tracking accuracy. FLC-based MPPT has evolved into a very popular topic, with many variations of FLC for MPPT being introduced in literature; For instance, various papers have considered using dP/dV as the input to the FLC. Specifically, Ref. 21 investigated and compared the performance in terms of tracking accuracy and convergence speed depending on the fuzzy rule base applied and hence determined the optimal rule variables and ranges. Reference 22 proposed a novel MPPT method based on a fuzzy logic controller (FLC) and applied it to a standalone photovoltaic system. This method uses a sampling measure of the PV array power and voltage, then determines the optimal increment required to obtain the optimal operating voltage, thereby permitting MPPT. References 23, 24 proposed using the change in power and the change in current as the two inputs to the FLC. However, the cited studies used many rules (between approximately 16 and 49) as well as membership functions defined for linguistic subsets due to their use of two inputs for the FLC.

By using a reduced number of fuzzy rules, the reduced-rule compressed fuzzy logic control (RR-FLC) proposed herein offers much lower computational demands, less system complexity, and simpler implementation. However, the primary drawback of this method is the requirement to calculate the angle conductance and angle of increment of conductance, which is more difficult than the conventional use of the direct PV current and voltage as the inputs of the FLC.

This research focuses on implementation of the incremental conductance (Inc. Cond.) and reduced-rule compressed fuzzy logic control (RR-FLC) MPPT methods to determine the MPP of a PV system and a detailed comparison between them in terms of tracking efficiency, convergence speed, implementation complexity, and cost. The remainder of this manuscript is organized as follows: "PV Cell Materials" section discusses different kinds of PV cell materials used for photoelectric generation and surveys their efficiency. "Equivalent Circuit Model of a PV Cell" section presents modeling of PV cells and panels using an equivalent circuit model. "MPPT for PV Panels" section discusses the mechanisms of the Inc. Cond. and RR-FLC MPPT methods. "Simulation Results for the MPPT Methods and Discussion" section reports experimental results and comparisons between the Inc. Cond. and RR-FLC MPPT methods. Finally, the conclusions of the study are presented in "Conclusions" section.

PV CELL MATERIALS

A solar cell, also called a PV cell, is a device that can produce a voltage difference when a source of light shines on it. The choice of the PV cell material plays an important role in the design and performance of such systems. PV cell materials include silicon, gallium arsenide (GaAs), copper indium diselenide ($CuInSe_2$), cadmium telluride (CdTe), indium phosphide, and many others, having different cell efficiencies and costs.[25,26]

PV cell technologies can be divided into two basic types: wafer-based PV (called first-generation PV) and thin-film cell PV (called second-generation PV). The first category includes crystalline silicon (c-Si) cells (both mono- and polycrystalline silicon) and gallium arsenide (GaAs) cells.[27] The conversion efficiency of monocrystalline cells is generally higher than that of polycrystalline cells, that is, 16% to 22% and 14% to 18%, respectively.[25] Thin-film technology (second-generation PV) provides alternative absorber materials, such as amorphous silicon (a-Si) or a combination or amorphous and microcrystalline silicon (a-Si/μc-Si), the compound semiconductor cadmium telluride (CdTe), and compound semiconductors made of copper, indium, gallium, and selenium (CIS or CIGS).[27] The conversion efficiencies of thin-film materials are approximately 7% to 9% for amorphous silicon (a-Si), 10% to 15% for cadmium telluride (CdTe), and 7% to 12% for copper indium gallium selenide. Another recent technology is dye-sensitized PV cells, currently achieving a highest laboratory efficiency of 12.3% on glass substrate and 8.6% on flexible stainless-steel substrate.[25]

In several studies, energy conversion efficiencies of approximately 40% have been achieved in laboratories by using III–V semiconductor compounds as PV materials. These types of PV cell achieve the highest energy conversion efficiency, rather than other materials such as silicon.[28] In addition to the potential for such high efficiency, III–V semiconductor compound materials offer advantages including bandgap tunability by tailoring the elemental composition, higher photon absorption based on their direct bandgap, greater robustness to high-energy rays for use in space applications, and less efficiency degradation by heat compared with Si PV cells.[29] Multistacking of PV materials with different bandgap energies is commonly used to obtain high-efficiency III–V PV cells, which are known as multijunction or tandem cells, to reduce the energy loss between the photon energy and the bandgap energy of the PV material and to absorb the energy in the solar spectrum over a wider wavelength range and more efficiently. Moreover, perovskite solar cells (PSCs) have recently emerged as a strong contender for next-generation photovoltaic technology and have attracted attention from the photovoltaic community, including both scientists and industry. "Perovskite" refers to the absorber material of PSC devices, which adopts the ABX_3 crystal structure.[30] In a few years, perovskite tandem solar cells have reached efficiencies above 25%.[31]

EQUIVALENT CIRCUIT MODEL OF A PV CELL

PV cells are the basic building blocks of PV systems, enabling direct transformation of sunlight into electricity. PV systems are made up of a number of individual PV cells connected in series to form strings and then in parallel to form modules.[19,32] Under light illumination, a PV cell acts as a current source. Electrons from the cell are excited to higher energy levels when a collision with a photon occurs. These electrons are free to move across the junction, creating a current that can be modeled as a photogenerated current source (I_{ph}). The characteristics of a PV array can be simulated using an ideal single-diode model as shown in Fig. 1.[33,34]

This ideal equivalent circuit model will offer a good compromise between accuracy and simplicity and be accurate enough to understand the PV characteristics.[34,35] The PV load current shown in Fig. 1 is defined as

$$I = I_{ph} - I_0\left(e^{\frac{q(V+R_sI)}{AkT}} - 1\right) - \frac{V + R_sI}{R_{sh}}, \qquad (1)$$

where I and V represent the output current and voltage of the PV cell, R_s and R_{sh} are the series and shunt resistance of the PV cell, respectively, I_{ph} is the photocurrent of the PV cell, I_0 is the diode saturation current, A is the diode quality factor ($\cong 1.2$), k is the Boltzmann constant (1.38×10^{-23} J/K), and T is the temperature of the PV cell in kelvin.[36]

By solving Eq. 1 or using the equivalent circuit model shown in Fig. 1, the electrical characteristic curves of a 150-W PV panel can be obtained in MATLAB for any environmental conditions. Under uniform conditions, only one maximum point is observed in the characteristic power curves. However, when the solar irradiance or temperature varies, the power generated by the PV module changes and the maximum point varies accordingly,[8] as illustrated by the voltage–power characteristic curves in Fig. 2 for different environmental conditions (solar irradiance and temperature).

When changing the levels of solar irradiance and/or temperature, the corresponding power–voltage curve of the PV panel also varies, and therefore the maximum power point. Figure 2 shows the power–voltage characteristic curves of the PV panel under different solar irradiance and temperature conditions. As shown in Fig. 2, the power of the PV panel is almost proportional to the solar irradiance. Hence, when the solar irradiance increases, the maximum power of the PV panel also increases. In addition, the power of the PV panel depends inversely on temperature, increasing as the temperature decreases.

MPPT FOR PV PANELS

With the changing direction of the sun, variations in the solar irradiance level and temperature result in changes in the power output of a PV cell. Therefore, PV cells and panels operate at a different power level depending on the environmental condition and electrical load. The nonlinear current–voltage (I–V) characteristics given by Eq. 1 clearly

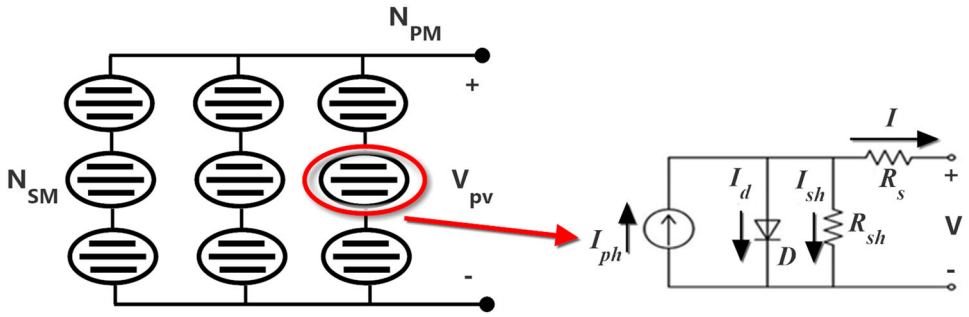

Fig. 1. PV panel and equivalent circuit model of PV cell.

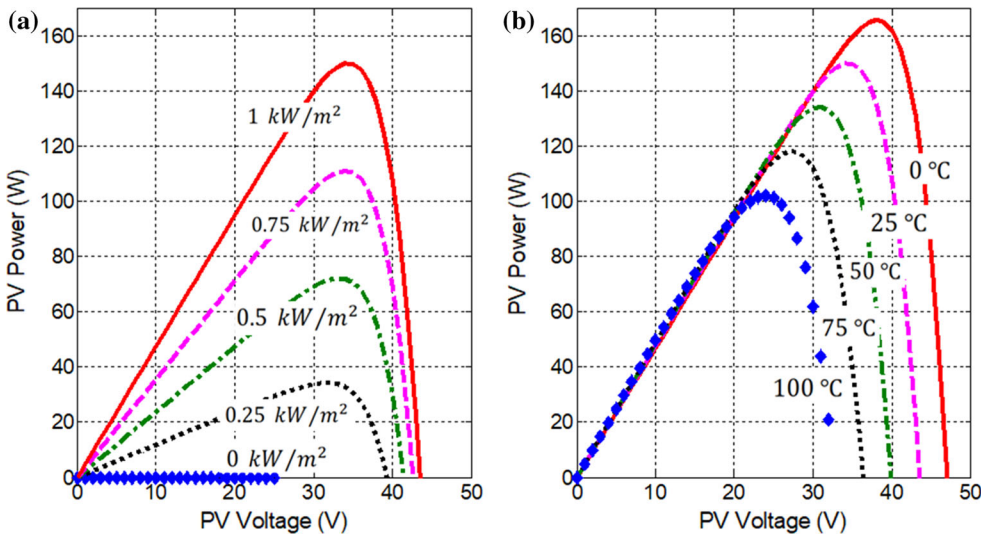

Fig. 2. Voltage and power curves of PV panel under different (a) solar irradiance and (b) temperature conditions.

display this variation under different temperature and solar irradiance conditions. The power–voltage (*P–V*) curve of a PV panel has a single maximum point, revealed as a peak in the power corresponding to a certain voltage (known as the MPP voltage) and current (known as the MPP current).[25] Therefore, there is a single optimum operating point for each combination of temperature and solar irradiance, at which the maximum output power can be obtained (Fig. 2).[35] This unique operating point is known as the maximum power point (MPP). In this context, to operate PV panels at the MPP, maximum-power-point tracking (MPPT) algorithms have been developed and implemented by researchers in literature.[37,38] MPPT aims to ensure that, under any environmental conditions, i.e., solar irradiance or temperature, the maximum achievable power is extracted from a PV system.[39–41] Figure 3 illustrates the MPP, at which the PV panel operates at maximum efficiency for a specific environmental condition.

To accomplish MPPT for a 150-W PV system, two different methods are considered herein, and their tracking accuracy and response rate compared. The

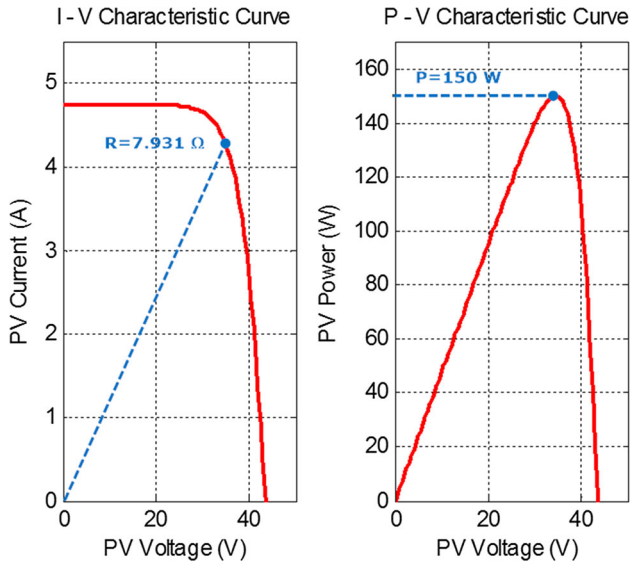

Fig. 3. *I–V* (current–voltage) and *P–V* (power–voltage) curves for electrical load value corresponding to the maximum power.

first method is the incremental conductance (Inc. Cond.) method, which operates by periodically incrementing or decrementing the output voltage of the PV panel and comparing the change in the output power. The second method uses reduced-rule compressed fuzzy logic control (RR-FLC) to determine the MPP point for uniform environmental conditions.

In certain situations, PV cells or panels may be exposed to different amounts of solar irradiance, which is referred to as a partial shading condition. Shading may be caused by features such as clouds, adjacent structures, or trees. Under such conditions, the less illuminated cells of the panel in the PV system dissipate some of the power generated by the others. In the resulting power–voltage characteristic curve, multiple local MPPs and a single global MPP occur due to the bypass diodes of the PV cells. When this occurs, conventional MPPT methods such as P&O and Inc. Cond. cannot distinguish the global MPP from local MPPs. Although they are efficient under uniform environmental conditions, they can fail to track the MPP under partial shading conditions. Due to this drawback of conventional MPPTs, intelligent MPPT methods such as particle swarm optimization (PSO), modified FLCs, artificial neural network (ANN), etc. are preferred to find the global MPP. Intelligent MPPTs include methods based on numerical computing and optimization, segmentation, and artificial intelligence. Although these methods can track the global MPP faster and more efficiently in partial shading conditions, their implementation is more complex and requires a more expensive digital controller compared with conventional MPPT approaches.[3,8]

Table I presents a comparison of conventional and intelligent MPPT methods in terms of their tracking efficiency in partial shading conditions, complexity, and implementation cost.

Incremental Conductance MPPT Method

The Inc. Cond. method tracks the MPP by comparing the sum of the incremental conductance plus the instantaneous conductance of a PV panel with zero, using the slope of the I–V characteristic of the PV system to track the MPP. This method is based on the principle that the slope of the power curve (dP/dV) of the PV system is zero at the MPP, positive when the output voltage is less than the MPP voltage (which means that the operating point is to the left of the MPP), and negative when the output voltage is greater than the MPP voltage (which means that the operating point is to the right of the MPP).[42] This explanation can be illustrated using the following simple equations:

$$\frac{dP}{dV} = \frac{d(V \times I)}{dV} = I + V\frac{dI}{dV} = 0, \tag{2}$$

$$\frac{\Delta I}{\Delta V} = -\frac{I}{V} \Rightarrow \text{MPP}, \tag{3}$$

$$\frac{\Delta I}{\Delta V} > -\frac{I}{V} \Rightarrow \text{left of MPP}, \tag{4}$$

$$\frac{\Delta I}{\Delta V} < -\frac{I}{V} \Rightarrow \text{right of MPP}. \tag{5}$$

Because it uses the differential of the operating point (dP/dV), the Inc. Cond. method can easily track the MPP in the case of rapidly changing environmental conditions (solar irradiance and temperature).[43] The accuracy and rapidity with which this method tracks the MPP depend on the size of the increment of the reference voltage.[32] A flowchart for the Inc. Cond. method is illustrated in Fig. 4.

The main advantages of this method are that it is convenient for any PV panel or array under uniform (no shading) environmental conditions, and that it requires no information regarding the PV system. In addition, the Inc. Cond. method requires current and voltage sensors to achieve MPPT, and it is simple to implement on a digital controller. Unfortunately, this method has the disadvantage of oscillating around the MPP, which decreases its efficiency, and it cannot work well under partial shading conditions.[8,20] However, variable-step-size

Table I. Comparison of conventional and intelligent MPPT methods in partial shading conditions

MPPT method	Tracking rate	Tracking efficiency	Complexity	Implementation cost
Conventional MPPT				
Perturb and observe (P&O)	Low	Low	Low	Low
Incremental conductance (Inc. Cond.)	Low	Low	Low	Low
Intelligent MPPT				
Particle swarm optimization (PSO)	Medium	Medium	High	High
Fuzzy logic control (FLC)	Medium	High	High	High
Artificial neural network (ANN)	High	High	High	High

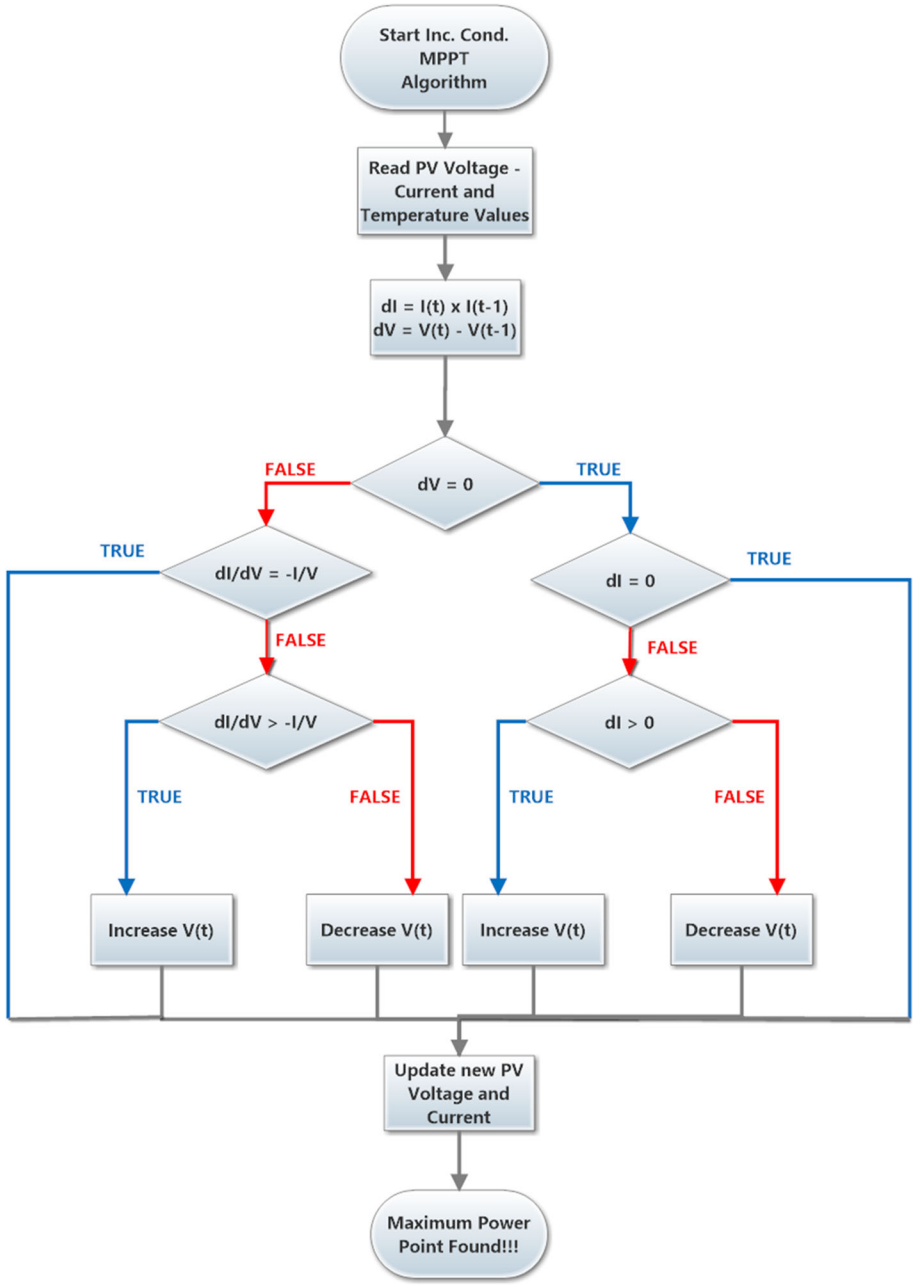

Fig. 4. Flowchart for Inc. Cond. method.

Inc. Cond. method implementations have also been studied in literature to reduce the oscillations around the MPP and thereby improve the tracking response;[44,45] For instance, Ref. 44 proposed a modified variable-step-size Inc. Cond. method that automatically adjusts the step size to track the MPP of a PV array. Reference 46 investigated modifications of the step size for P&O and Inc. Cond. methods to improve their dynamic and steady-state MPPT performance. Reference 47 presented a novel variable-step-size incremental resistance MPPT algorithm that not only has the merits of Inc. Cond. but also automatically adjusts the step size to track the MPP of the PV array.

Reduced-Rule Compressed Fuzzy Logic Control MPPT Method

Fuzzy logic control (FLC)-based MPPT is one of the most widely used methods to achieve MPPT for any PV system in any environmental conditions. FLCs offer several advantages including better performance, robustness, and simple design. In addition, such methods do not require knowledge about the exact model of the system.[48,49] The main

advantage of fuzzy control methods is their good performance under fast-changing weather conditions, although they require a high-cost processor and difficult acquisition of empirical data.[50]

In this method, variables adopt various nonnumeric and linguistic values, e.g., "high," "low," "medium," and "often."[51] FLCs operate using membership functions instead of a mathematical model. FLCs can be divided into three parts, viz. fuzzification, fuzzy inference, and defuzzification. During fuzzification, the input variable(s) are converted into linguistic variables according to chosen membership functions. In the inference stage, the linguistic variables are manipulated based on a fuzzy rule table, which defines the behavior of the MPPT control. In the defuzzification stage, the FLC output is converted from a linguistic to a numerical value using the corresponding membership function.[52]

In the proposed RR-FLC method, a single input variable is used to control the MPPT process of a PV system. The input of the RR-FLC is the sum of the angle conductance $[\theta_1 = \tan^{-1}(I_{pv}/V_{pv})]$ and the angle of increment of conductance $[\theta_2 = \tan^{-1}(\mathrm{d}I_{pv}/\mathrm{d}V_{pv})]$ as described by Eq. 6.

$$\theta_1 = \tan^{-1}\left(\frac{I_{pv}}{V_{pv}}\right), \quad \tan\theta_1 = \frac{I_{pv}}{V_{pv}}, \quad \text{and}$$
$$\theta_2 = \tan^{-1}\left(\frac{\mathrm{d}I_{pv}}{\mathrm{d}V_{pv}}\right), \quad \tan\theta_2 = \frac{\mathrm{d}I_{pv}}{\mathrm{d}V_{pv}}. \tag{6}$$

The slope of the power curve ($\mathrm{d}P/\mathrm{d}V$) of the PV system is zero at the MPP. Therefore, Eq. 3 can be rewritten in terms of the angle conductance and angle of increment of conductance parameters as shown in Eq. 7.

$$\frac{dP_{pv}}{dV_{pv}} = \frac{d(V_{pv} \times I_{pv})}{dV_{pv}} = I_{pv} + V_{pv}\frac{dI_{pv}}{dV_{pv}} = \frac{I_{pv}}{V_{pv}} + \frac{dI_{pv}}{dV_{pv}}$$
$$= \tan\theta_1 + \tan\theta_2 = 0 \tag{7}$$

$$\tan(\theta_1 + \theta_2) = \frac{\tan(\theta_1) + \tan(\theta_2)}{1 - \tan\theta_1 \tan\theta_2} = \frac{\frac{I_{pv}}{V_{pv}} + \frac{\mathrm{d}I_{pv}}{\mathrm{d}V_{pv}}}{1 - \frac{I_{pv}}{V_{pv}}\frac{\mathrm{d}I_{pv}}{\mathrm{d}V_{pv}}} = 0. \tag{8}$$

Using Eqs. 7 and 8, the sum of the angle conductance and angle of increment of conductance $(\theta_1 + \theta_2)$, which is used as the input of the RR-FLC MPPT method, must be equal to zero around the MPP, i.e.,

$$\theta_1 + \theta_2 = \tan^{-1}\left(\frac{I_{pv}}{V_{pv}}\right) + \tan^{-1}\left(\frac{\mathrm{d}I_{pv}}{\mathrm{d}V_{pv}}\right) = 0. \tag{9}$$

The relationships between $\theta_1 + \theta_2$ and the current–voltage and power–voltage characteristic curves of the PV panel are illustrated in Fig. 5a and b, respectively.

As seen in Eq. 9 and Fig. 5b, the sum of the angles of the PV panel conductance and increment of conductance equals zero around the MPP. Therefore, the membership functions of the input and the rule base set for the fuzzy inference system of the RR-FLC MPPT must be identified according to this condition. The flowchart for the RR-FLC method is illustrated in Fig. 6.

The proposed RR-FLC to control the MPPT process has three stages, known as fuzzification, inference, and defuzzification. In the fuzzification stage, the input variable, i.e., the sum of the angles $(\theta_1 + \theta_2)$, is assigned to several linguistic variables; the corresponding membership functions are shown in Fig. 6, denoted by NB (negative big), NS (negative small), ZE (zero), PS (positive small), and PB (positive big). In the inference stage, these linguistic variables are manipulated based on a fuzzy rule table. In the defuzzification stage, the RR-FLC output is converted from a linguistic to a numerical value using the membership function, defining the output. Hence, the number of corresponding fuzzy rules is decreased to five by using a single input $(\theta_1 + \theta_2)$ for the RR-FLC. The corresponding fuzzy rule set is shown in Fig. 7.

In literature, most conventional FLC methods require two input variables. Generally, each input requires several linguistic variables. This makes FLCs more complex and highly computationally demanding. Thus, the corresponding fuzzy rule tables consist of many rules, i.e., many more than five.[1,2,4,48,53] Use of the method proposed herein when designing the output domains allows greater step sizes, thereby improving the efficiency of the MPPT algorithm. The other advantage is that this algorithm does not require use of a second set of MPPT input variables.[54] Since RR-FLC- and FLC-based MPPT functions are based on the derivative of the power and voltage ratio, they cannot detect the true global MPP for partial shading conditions and must be modified and adapted using the input variables and fuzzy rules to effectively track the global MPP of a PV system.[3]

SIMULATION RESULTS FOR THE MPPT METHODS AND DISCUSSION

In this study, the tracking performance and accuracy of the Inc. Cond. and RR-FLC methods were compared using MATLAB simulations. The Inc. Cond. method is based on a comparison of how the voltage and current change and tracks the MPP by changing the operating PV voltage depending on a chosen voltage step size. In this study, a relatively large step size (3.5 V) as well as a smaller step size (0.5 V) were chosen to highlight the resulting differences in tracking performance and convergence speed. Additionally, the range of membership functions of the RR-FLC was adjusted to 3.5 V for

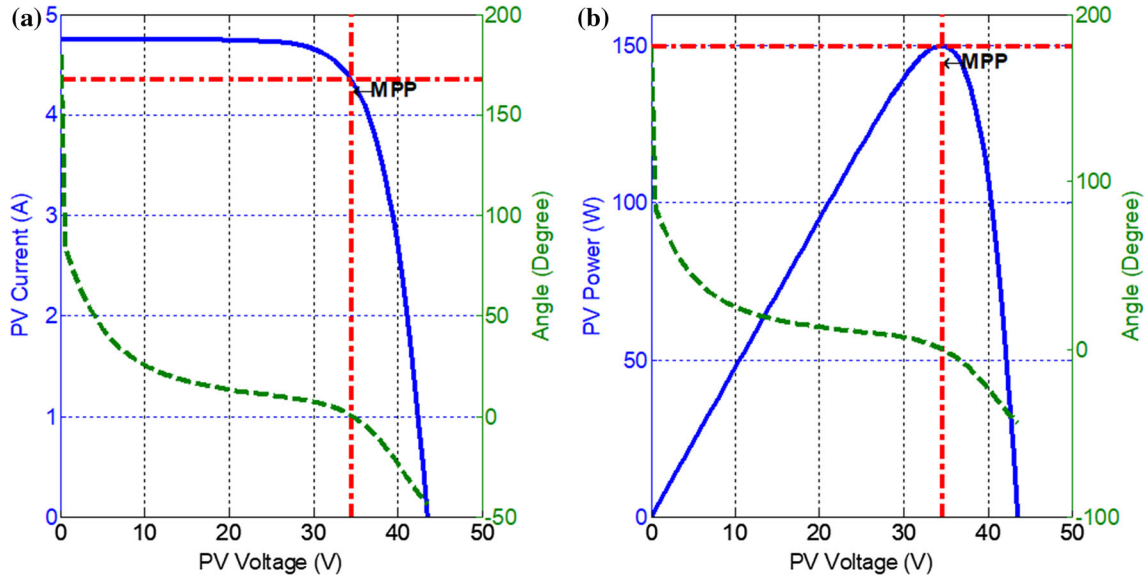

Fig. 5. (a) Current–voltage of PV panel and the corresponding sum of angle conductance and angle of increment of conductance characteristic curves. (b) Power–voltage of PV panel and the corresponding sum of angle conductance and angle of increment of conductance characteristic curves.

comparison with the Inc. Cond. method with the same step size.

The performance results for the Inc. Cond. method with step size of 0.5 V and 3.5 V as well as the RR-FLC control method are shown in Fig. 8 for standard test conditions (1 kW/m^2, 25°C).

As shown in Fig. 8, the Inc. Cond. MPPT method with step size of 3.5 V showed the best response iteration rate but worst accuracy performance due to the larger oscillations around the MPP. The tracking speed for the Inc. Cond. (3.5 V), Inc. Cond. (0.5 V), and RR-FLC method was 11, 68, and 45 iterations, respectively. According to these results, the iteration rate of the Inc. Cond. (3.5 V) method was 6.18 (68/11) times faster than the Inc. Cond. (0.5 V) method and 4.09 (45/11) times faster than the RR-FLC method. In the standard test condition, the maximum power of the PV panel is 150 W. Nevertheless, the Inc. Cond. (3.5 V) found a maximum power of 142.988 W. Therefore, the accuracy of this this method is approximately 95.33%, worse than that of the Inc. Cond. (0.5 V) or RR-FLC MPPT method. The simulation results in terms of response iteration rate, tracking performance and efficiency, tracking speed, complexity, and implementation cost are presented and compared in Table II.

Although Inc. Cond. methods are easier to implement and have low costs, their tracking efficiency and performance are not as good as those obtained using the RR-FLC method. In addition, the tracking speed of the Inc. Cond. methods varies with the parameters used to obtain the reference voltage, and they cannot find the global MPP in partial shading conditions. Although the RR-FLC also cannot track the global MPP, this can be achieved by modifying the fuzzy linguistic variables and rules for partial shading conditions.

The generated energy can be calculated from Fig. 8 using the generated power and time duration. Each iteration requires some time, which depends on the clock frequency of the processor and the code written to accomplish the task. Therefore, an iteration is taken as a unit to calculate the energy. The energy obtained at the end of the simulation of the PV panel under the standard test condition is shown in Fig. 9.

According to the results of these simulations, the RR-FLC MPPT method exhibited the best performance in terms of energy extraction. After 2000 iterations, the RR-FLC showed the best energy efficiency with 298.206 kW × iterations. The simulation results for the energy comparison are presented in Table III.

To highlight the performance of the RR-FLC MPPT method, simulation results for different solar irradiance values (1 kW/m^2, 0.8 kW/m^2, 0.6 kW/m^2, and 0.4 kW/m^2) at fixed temperature (30°C) are presented in Fig. 10. The Inc. Cond. (0.5 V) method exhibits better tracking efficiency than the Inc. Cond. (3.5 V) method but a slower response rate than the RR-FLC or Inc. Cond. (3.5 V) method. Additionally, the oscillations around the MPP remain. The RR-FLC method exhibits a better response rate than the Inc. Cond. (0.5 V) method, and the best tracking efficiency performance (99.99%). In addition, no oscillations around the MPP occur. Hence, the RR-FLC MPPT method offers an increase in the tracking efficiency performance by 4.66% compared with the Inc. Cond. MPPT method. Therefore, the RR-FLC method is

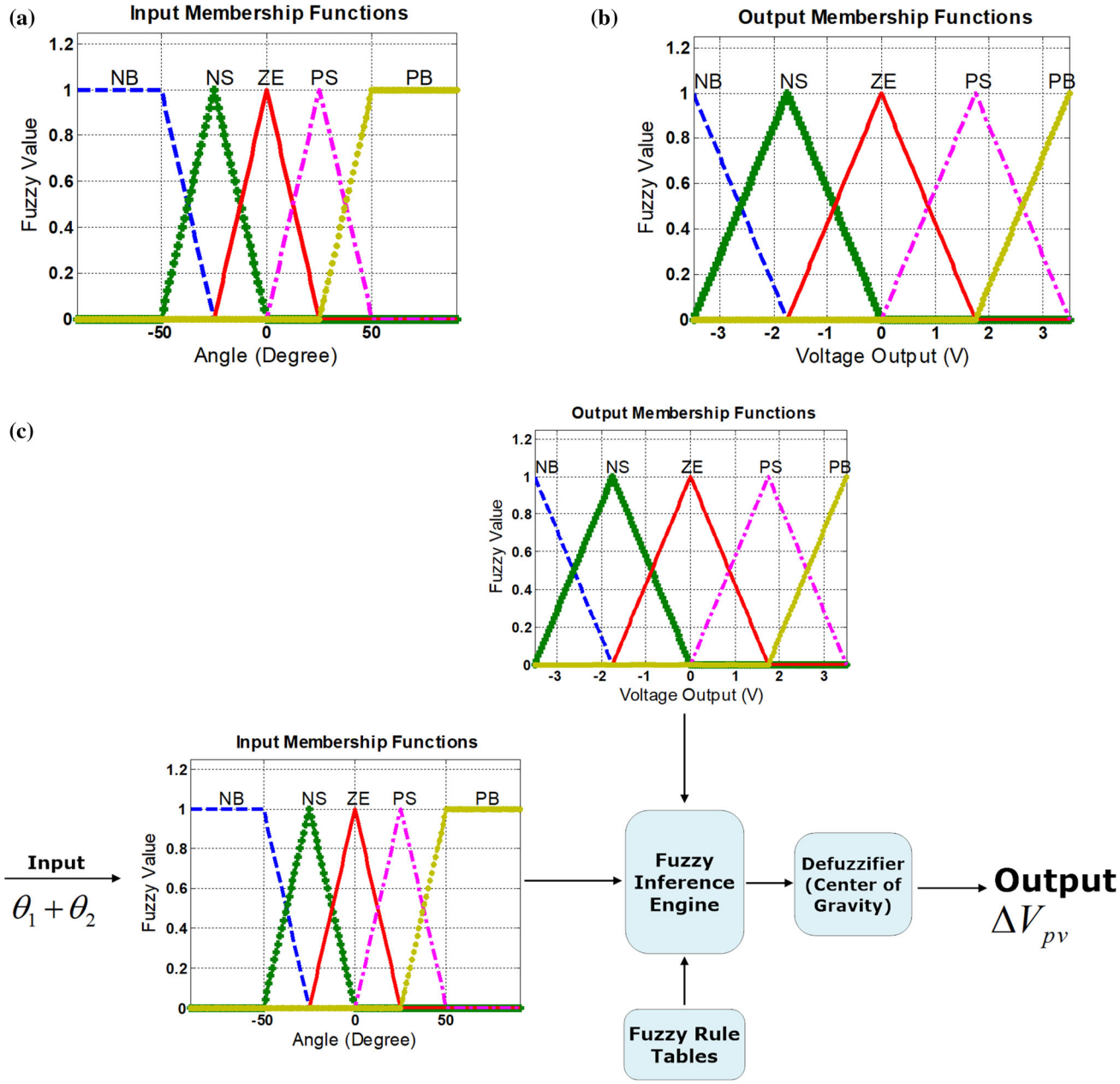

Fig. 6. (a) Input membership functions of the RR-FLC. (b) Output membership functions of the RR-FLC. (c) Flowchart for the RR-FLC.

more convenient for practical PV applications due to its enhanced tracking performance, fewer oscillations, and acceptable response rate compared with the Inc. Cond. method. In addition, the RR-FLC method requires fewer rules in the fuzzy rule table and is simpler than conventional FLC methods. Hence, the results of this study show that the proposed RR-FLC method represents a better option for MPPT due to its simplicity, response rate, and tracking performance compared with the Inc. Cond. and conventional FLC-based MPPT methods for uniform environmental conditions.

CONCLUSIONS

Generating power from photovoltaic systems has become popular, because they represent a sustainable, clean, and abundant generation technology. Hence, extraction of the maximum amount of available power has become an important issue for PV systems. Power generation by PV systems depends on atmospheric conditions such as solar irradiance and temperature. Thus, MPPT methods play an important role in operating PV systems at maximum efficiency under atmospheric changes. In literature, researchers have developed various

(a)

$\theta_1 + \theta_2$	NB	NS	ZE	PS	PB
ΔV_{pv}	NB	NS	ZE	PS	PB
Region Area	Region 1		Region 2	Region 3	

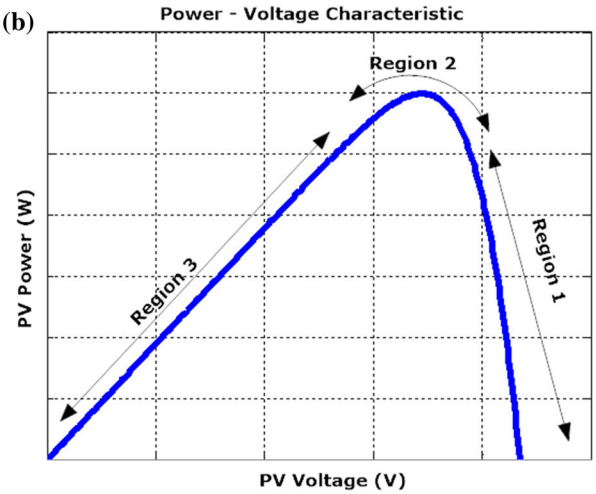

Fig. 7. (a) Fuzzy rules for the defined linguistic variables for the RR-FLC. (b) PV power–voltage and angle MPPT diagram for proposed RR-FLC-based MPPT method.

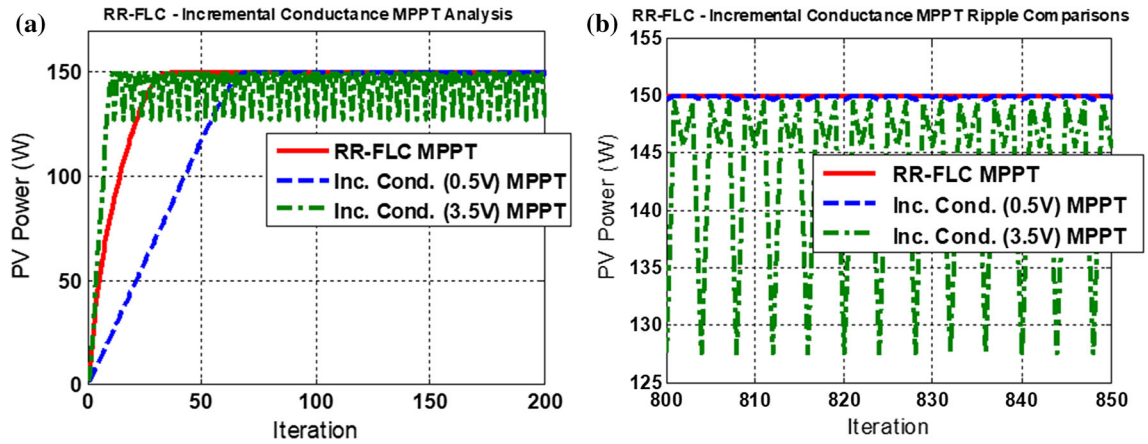

Fig. 8. Performance of Inc. Cond. and RR-FLC MPPT methods under standard test conditions (1 kW/m^2, 25°C): (a) PV power curves, (b) close-up of oscillations.

Table II. Comparison of Inc. Cond. and RR-FLC MPPT methods

MPPT type	Iteration rate	MPP power (W)	Tracking accuracy (%)	Tracking rate	Tracking efficiency	Complexity	Implementation cost
Inc. Cond. (3.5 V)	11	142.988	95.33	High	Low	Low	Low
Inc. Cond. (0.5 V)	68	149.862	99.91	Low	Medium	Low	Low
RR-FLC	45	149.987	99.99	Medium	High	High	High

MPPT methods to identify the optimum operating point at which PV panels can extract the maximum available power for the current conditions. In this study, a traditional Inc. Cond. method with different step sizes was compared with a method based on reduced-rule compressed fuzzy logic control (RR-FLC) that requires only a single input and less computing power than conventional FLC-based MPPT methods. The performance of the different MPPT methods under uniform environmental conditions was investigated and compared. The tracking accuracy and performance efficiency are discussed in detail based on MATLAB simulations for a 150-W PV panel. The results of the simulations reveal that the RR-FLC MPPT method exhibits a fast response rate, no oscillations around the MPP, and better tracking accuracy, and is more convenient than the Inc. Cond. MPPT method. The RR-FLC MPPT method achieves an improvement in the tracking accuracy of 4.66% compared with the Inc.

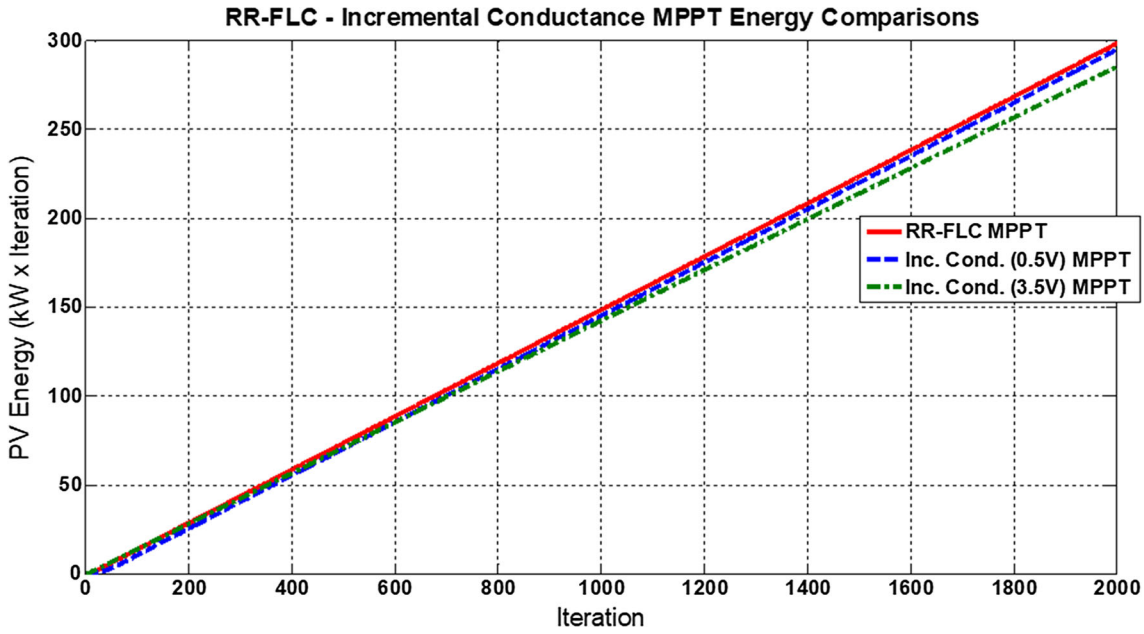

Fig. 9. Energy obtained from the PV panel under standard test condition.

Table III. Comparison of energy results for Inc. Cond. and RR-FLC MPPT methods

MPPT type	MPP energy (kW × iterations)	Energy efficiency (%)
Inc. Cond. (3.5 V)	258.148	95.05
Inc. Cond. (0.5 V)	294.812	98.27
RR-FLC	298.206	99.40

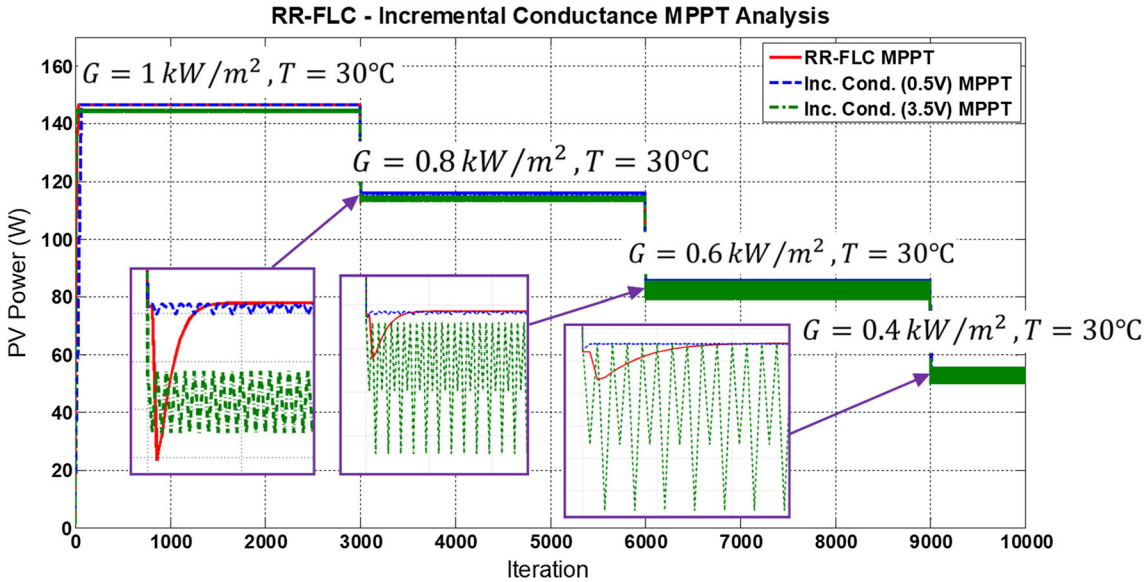

Fig. 10. PV power curves under different solar irradiance values at fixed temperature (30°C).

Cond. MPPT method under the standard test condition. Hence, it can be concluded that both MPPT methods provide the maximum power for actual atmospheric conditions, but the tracking performance and response rate of the RR-FLC MPPT method are more appropriate for uniform environmental conditions due to its simplicity and the lack of oscillations around the MPP.

REFERENCES

1. T.H. Kwan and X. Wu, *Sol. Energy* 137, 189 (2016).
2. H. Bounechba, A. Bouzid, K. Nabti, and H. Benalla, *Energy Procedia* 50, 677 (2014).
3. A.R. Jordehi, *Renew. Sustain. Energy Rev.* 65, 1127 (2016).
4. F. Chekired, C. Larbes, D. Rekioua, and F. Haddad, *Energy Procedia* 6, 541 (2011).
5. T. Radjai, L. Rahmani, S. Mekhilef, and J.P. Gaubert, *Sol. Energy* 110, 325 (2014).
6. H. Rezk and A.M. Eltamaly, *Sol. Energy* 112, 1 (2015).
7. Z. Cheng, H. Yang, and Y. Sun, in *Seventh International Conference on Fuzzy Systems and Knowledge Discovery* (2010), pp. 1244–1248.
8. E. Kandemir, N.S. Cetin, and S. Borekci, *Renew. Sustain. Energy Rev.* 78, 93 (2017).
9. Z. Salam, J. Ahmed, and B.S. Merugu, *Appl. Energy* 107, 135 (2013).
10. T. Esram, P.L. Chapman, and I.E.E.E. Trans, *Energy Convers.* 22, 439 (2007).
11. M.A.G. de Brito, L. Galotto, L.P. Sampaio, G.D.A. e Melo, and C.A. Canesin, *IEEE Trans. Ind. Electron.* 60, 1156 (2013).
12. W. Xiao, A. Elnosh, V. Khadkikar, and H. Zeineldin, in *37th Annual Conference of the IEEE Industrial Electronics Society* (2011), pp. 3900–3905.
13. B. Subudhi and R. Pradhan, *IEEE Trans. Sustain. Energy* 4, 89 (2013).
14. M.A. Elgendy, B. Zahawi, and D.J. Atkinson, *IEEE Trans. Sustain. Energy* 4, 108 (2013).
15. R.I. Putri, S. Wibowo, and M. Rifa'i, *Energy Procedia* 68, 22 (2015).
16. S.R. Chafle and U.B. Vaidya, *Int. J. Adv. Res. Electr. Electron. Instrum. Eng.* 2, 2719 (2013).
17. P. Suwannatrai, P. Liutanakul, and P. Wipasuramonton, in *The 8th Electrical Engineering/Electronics, Computer, Telecommunications and Information Technology (ECTI) Association of Thailand—Conference* (2011), pp. 637–640.
18. A. Safari and S. Mekhilef, in *24th Canadian Conference on Electrical and Computer Engineering (CCECE)* (2011), pp. 000345–000347.
19. S. Lyden and M.E. Haque, *Renew. Sustain. Energy Rev.* 52, 1504 (2015).
20. D. Sera, L. Mathe, T. Kerekes, S.V. Spataru, and R. Teodorescu, *IEEE J. Photovolt.* 3, 1070 (2013).
21. S. Hajighorbani, M.A.M. Radzi, M.Z.A. Ab Kadir, S. Shafie, R. Khanaki, and M.R. Maghami, *Int. J. Photoenergy* 2014, 1 (2014).
22. S. Lalouni, D. Rekioua, T. Rekioua, and E. Matagne, *J. Power Sources* 193, 899 (2009).
23. B. Alajmi, K.H. Ahmed, S.J. Finney, and B. Williams, *IEEE Trans. Power Electron.* 26, 1022 (2011).
24. B.N. Alajmi, K.H. Ahmed, S.J. Finney, and B.W. Williams, *IEEE Trans. Ind. Electron.* 60, 1596 (2013).
25. M.M. Fouad, L.A. Shihata, and E.I. Morgan, *Renew. Sustain. Energy Rev.* 80, 1499 (2017).
26. S. Mekhilef, R. Saidur, and M. Kamalisarvestani, *Renew. Sustain. Energy Rev.* 16, 2920 (2012).
27. E. Płaczek-Popko, *Opto-Electronics Rev.* 25, 55 (2017).
28. M.A. Green, Y. Hishikawa, W. Warta, E.D. Dunlop, D.H. Levi, J.H. Ebinger, and A.W.H. Ho-Baille, *Prog. Photovolt. Res. Appl.* 25, 668 (2017).
29. K. Tanabe, *Energies* 2, 504 (2009).
30. H.J. Snaith, *J. Phys. Chem. Lett.* 4, 3623 (2013).
31. J. Werner, B. Niesen, and C. Ballif, *Adv. Mater. Interfaces* 5, 1700731 (2018).
32. A. Belkaid, I. Colak, and O. Isik, *Appl. Energy* 179, 523 (2016).
33. J. Li and H. Wang, in *International Conference on Sustainable Power Generation and Supply* (2009), pp. 1–6.
34. M.Y. Javed, A.F. Murtaza, Q. Ling, S. Qamar, and M.M. Gulzar, *Energy Build.* 133, 59 (2016).
35. A. Amir, A. Amir, J. Selvaraj, and N.A. Rahim, *Renew. Sustain. Energy Rev.* 62, 350 (2016).
36. E. Kandemir, N.S. Cetin, and S. Borekci, *Period. Eng. Nat. Sci.* 5, 16 (2017).
37. Y.-C. Kuo, T.-J. Liang, and J.-F. Chen, *IEEE Trans. Ind. Electron.* 48, 594 (2001).
38. Y. Zou, Y. Yu, Y. Zhang, and J. Lu, *Procedia Eng.* 29, 105 (2012).
39. N. Bizon, *Renew. Sustain. Energy Rev.* 57, 524 (2016).
40. A. Kheldoun, R. Bradai, R. Boukenoui, and A. Mellit, *Energy Convers. Manag.* 111, 125 (2016).
41. S. Palani, S. Peddapati, K. Sundareswaran, and I.E.T. Renew, *Power Gener.* 8, 670 (2014).
42. A. Gupta, Y.K. Chauhan, and R.K. Pachauri, *Sol. Energy* 136, 236 (2016).
43. D.C. Huynh and M.W. Dunnigan, *IEEE Trans. Sustain. Energy* 7, 1421 (2016).
44. Fangrui Liu, Shanxu Duan, Fei Liu, Bangyin Liu, and Yong Kang, *IEEE Trans. Ind. Electron.* 55, 2622 (2008).
45. Y.-H. Ji, D.-Y. Jung, J.-G. Kim, J.-H. Kim, T.-W. Lee, and C.-Y. Won, *IEEE Trans. Power Electron.* 26, 1001 (2011).
46. A. Pandey, N. Dasgupta, and A. K. Mukerjee, in *32nd Annual Conference on IEEE Industrial Electronics (IECON)* (2006), pp. 4387–4391.
47. Q. Mei, M. Shan, L. Liu, and J.M. Guerrero, *IEEE Trans. Ind. Electron.* 58, 2427 (2011).
48. P. Takun, S. Kaitwanidvilai, and C. Jettanasen, in *Proceedings of the International MultiConference of Engineers and Computer Scientists* (2011).
49. C.S. Chiu and I.E.E.E. Trans, *Energy Convers.* 25, 1123 (2010).
50. S. Li, H. Liao, H. Yuan, Q. Ai, and K. Chen, *Sol. Energy* 144, 175 (2017).
51. Syafaruddin, E. Karatepe, T. Hiyama, and I.E.T. Renew, *Power Gener.* 3, 239 (2009).
52. S. Saravanan and N. Ramesh Babu, *Renew. Sustain. Energy Rev.* 57, 192 (2016).
53. P.-C. Cheng, B.-R. Peng, Y.-H. Liu, Y.-S. Cheng, and J.-W. Huang, *Energies* 8, 5338 (2015).
54. J.-K. Shiau, Y.-C. Wei, and B.-C. Chen, *Algorithms* 8, 100 (2015).